


Article

Control of Sunroof Buffeting Noise by Optimizing the Flow Field Characteristics of a Commercial Vehicle

Rongjiang Tang ¹, Hongbin He ¹, Zengjun Lu ², Shenfang Li ^{1,*}, Enyong Xu ², Fei Xiao ² and Avelino Núñez-Delgado ³ 

¹ School of Mechanical and Electrical Engineering, Guilin University of Electronic Technology, Guilin 541004, China; tangrongjiang@guet.edu.cn (R.T.); hongbinhe_96@163.com (H.H.)

² Dong Feng Liuzhou Automobile Co., Ltd., Liuzhou 545005, China; luzj1@dfzm.com (Z.L.); xuey@dfzm.com (E.X.); xiaof@dfzm.com (F.X.)

³ Department of Soil Science and Agricultural Chemistry, Engineering Polytechnic School, University of Santiago de Compostela, Campus Universitario s/n, 27002 Lugo, Spain; avelino.nunez@usc.es

* Correspondence: 1801201025@mails.guet.edu.cn

Abstract: When a commercial vehicle is driving with the sunroof open, it is easy for the problem of sunroof buffeting noise to occur. This paper establishes the basis for the design of a commercial vehicle model that solves the problem of sunroof buffeting noise, which is based on computational fluid dynamics (CFD) numerical simulation technology. The large eddy simulation (LES) method was used to analyze the characteristics of the buffeting noise with different speed conditions while the sunroof was open. The simulation results showed that the small vortex generated in the cab forehead merges into a large vortex during the backward movement, and the turbulent vortex causes a resonance response in the cab cavity as the turbulent vortex moves above the sunroof and falls into the cab. Improving the flow field characteristics above the cab can reduce the sunroof buffeting noise. Focusing on the buffeting noise of commercial vehicles, it is proposed that the existing accessories, including sun visors and roof domes, are optimized to deal with the problem of sunroof buffeting noise. The sound pressure level of the sunroof buffeting noise was reduced by 6.7 dB after optimization. At the same time, the local pressure drag of the commercial vehicle was reduced, and the wind resistance coefficient was reduced by 1.55% compared to the original commercial vehicle. These results can be considered as relevant, with high potential applicability, within this field of research.



Citation: Tang, R.; He, H.; Lu, Z.; Li, S.; Xu, E.; Xiao, F.; Núñez-Delgado, A. Control of Sunroof Buffeting Noise by Optimizing the Flow Field Characteristics of a Commercial Vehicle. *Processes* **2021**, *9*, 1052. <https://doi.org/10.3390/pr9061052>

Academic Editor:
Krzysztof Rogowski

Received: 24 May 2021
Accepted: 10 June 2021
Published: 16 June 2021

Publisher's Note: MDPI stays neutral with regard to jurisdictional claims in published maps and institutional affiliations.



Copyright: © 2021 by the authors. Licensee MDPI, Basel, Switzerland. This article is an open access article distributed under the terms and conditions of the Creative Commons Attribution (CC BY) license (<https://creativecommons.org/licenses/by/4.0/>).

Keywords: sunroof buffeting noise; computational fluid dynamics; large eddy simulation; sun visor; roof dome; commercial vehicle

1. Introduction

Buffeting noise is the aerodynamic acoustic response when a vehicle is moving with the sunroof or side window opened, and it occurs due to the differences in the air inside the vehicle and the external transient airflow. The buffeting noise has a low frequency (less than 20 Hz) and a high sound pressure level (greater than 110 dB) [1]. The low-frequency pressure pulsation of the buffeting noise causes a strong sense of pressure on the ears, which can result in fatigue and unpleasant feelings for drivers and passengers in a short period. Staying in such an environment for a long-time could even cause damage to hearing [2,3]. Therefore, further research on the optimization of buffeting noise is needed to improve the acoustic comfort of vehicles.

In terms of buffeting noise research on the side windows of the vehicle, He [4] used the method of the vehicle aero-acoustic wind tunnel test to analyze the influence of different factors, including the spatial position of the car, wind speed, side window opening area, yaw angle, the different ways of opening side windows on the sound pressure level, and the frequency of the side window buffeting noise. Yang [5] also studied the side window

buffeting noise of a car, pointing out that when a single window is opened, the rear window buffeting noise is higher than that of the front window, and that different ways of opening the side windows can reduce the buffeting noise.

In the research on the sunroof buffeting noise, reducing the buffeting noise has always been the research focus of scholars. Oettle [6] used the Lattice Boltzmann method to evaluate the sunroof buffeting characteristics of a specific model of a vehicle, and the suppressing effect of the spoiler with or without the grid on the sunroof buffeting characteristics was analyzed. Wang [7] studied the mechanism of the sunroof buffeting noise at the speed of low Mach numbers based on a three-dimensional cavity model. The results showed that airflow separation, vortex shedding, vortex impact, periodic pressure wave feedback, and Helmholtz resonance are responsible for sunroof buffeting. Wang [8] studied the suppression effect of a serrated sunroof trailing edge on the sunroof buffeting noise, and pointed out that this strategy can break down the strong vortex into smaller eddies and effectively reduce the sound pressure level in the car.

With the development of CFD technology and convenient computing resources, numerical simulation methods have been widely used in the research on sunroof buffeting. Gu [9] used the LES method to calculate the side window buffeting noise near the driver while the side window was partially opened, and verified the correctness of the analysis results by a road test. Gong [10] analyzed the LES transient simulation model of an SUV-type vehicle to obtain the buffeting frequency and the sound pressure level on the passenger's left ear while the sunroof was opened. At the same time, the sound pressure level of the passenger's left ears was reduced by optimizing the skylight spoiler. He [11,12] studied the sunroof buffeting noise with different vehicle speeds based on the LES method, and designed a new type of baffle plate to reduce the sound pressure level of the sunroof buffeting noise. The existing wind buffeting noise control strategies include: adding aerodynamic accessories such as spoilers, grooves, and setting columns in the skylight or side window; adjusting the structure of the cab to stagger the resonance frequency; reducing the size of the turbulence vortex; and using sound wave superposition technology and jet flow technology to suppress the wind buffeting noise [13–15]. The cab of a commercial vehicle is a closed space, and it is easy for turbid air and uncomfortable odors in the cab to be produced. Installing skylights allows the air to circulate inside and outside the cab which can improve the air quality. As with passenger cars, there is still a need to install sunroofs in commercial vehicles. The current sunroof buffeting noise research has mainly focused on passenger vehicles, and little work has been conducted on heavy commercial vehicles. In addition, adding aerodynamic accessories will increase the cost and even affect the appearance of the vehicles. Due to the complexity of the wind buffeting noise, it is difficult to apply sound wave superposition technology and jet flow technology based on an active control strategy.

With the above information in mind, the proposed study uses the LES method to investigate the phenomenon and the formation mechanism of the sunroof buffeting noise while the sunroof is opened in a heavy commercial vehicle. A scheme of optimizing the existing accessories including a sun visor and a roof dome is proposed to improve the flow field above the roof and to reduce the sunroof buffeting noise. The results of this study could contribute to the optimization of the sunroof buffeting noise in commercial vehicles, which can be considered of relevance in this field of research. The remaining chapters are arranged as follows. In Section 2, some basic mathematical theories used in this paper are introduced. In Section 3, a simulation model for the sunroof buffeting noise of a commercial vehicle is established. Then, in Section 4, the sunroof buffeting noise characteristics at different driving conditions are analyzed. In Section 5, the optimization of the sunroof buffeting noise is discussed, and the wind resistance of the vehicle is analyzed. The last section is a summary of this paper.

2. Mathematical Methods

2.1. Large Eddy Simulation

The commercial vehicle cab is equal to a Helmholtz cavity (a cavity where air resonance takes place) while the sunroof is opened. The buffeting noise generated in this type of cavity is mainly a low-frequency discrete noise [16]. While the skylight is opened, the air flow is complex and irregular, making it highly nonlinear. Usually, large eddy simulations are used to analyze the transient flow field of such problems, as they are based on mathematical modelling for turbulence used in computational fluid dynamics. The basic governing equations for turbulence calculation are as follows [17]:

continuity equation

$$\frac{\partial \rho}{\partial t} + \frac{\partial \rho \bar{v}_i}{\partial x_i} = 0 \quad (1)$$

kinematic equation

$$\frac{\partial(\rho \bar{v}_i)}{\partial t} + \frac{\partial(\rho \bar{v}_i \bar{v}_j)}{\partial x_j} = -\frac{\partial \bar{p}}{\partial x_i} + \frac{\partial}{\partial x_j} \left(\mu \frac{\partial \bar{v}_i}{\partial x_j} \right) - \frac{\partial \tau_{ij}}{\partial x_j} \quad (2)$$

where t is the time, x_i and x_j are the coordinate axis components, ρ is the fluid density, \bar{v}_i and \bar{v}_j are the time-averaged velocity, \bar{p} is the air pressure, μ is the turbulent viscosity coefficient, and τ_{ij} is the sub-grid scale stress, all of which are expressed in the appropriate units.

Taking into account the fact that vortex identifiers can be used to build eddy-viscosity sub-grid scale models for large eddy simulation, in the current study the vortex viscous sub-grid model is introduced as follows:

$$\tau_{ij} - \frac{1}{3} \tau_{kk} \delta_{ij} = -2\mu_t \bar{S}_{ij} \quad (3)$$

$$\bar{S}_{ij} = \frac{1}{2} \left(\frac{\partial \bar{u}_i}{\partial x_j} + \frac{\partial \bar{u}_j}{\partial x_i} \right) \quad (4)$$

where δ_{ij} is the Kronecker delta, μ_t is the sub-grid scale stress turbulent viscosity, τ_{kk} is the iso-tropic sub-grid scale stress, and \bar{S}_{ij} is strain rate tensor. Once again, all of these values are expressed in the appropriate units.

2.2. Ffowcs Williams and Hawkings (FW-H) Equation

Based on the acoustic analogy theory proposed by Lighthill, Williams and Hawkins developed the FW-H equation, which is suitable for the moving solid's boundary and its differential form as follows [18]:

$$\left(\frac{1}{c^2} \frac{\partial^2}{\partial t^2} - \frac{\partial^2}{\partial x_i^2} \right) p' = \frac{\partial^2}{\partial x_i \partial x_j} [T_{ij} H(f)] - \frac{\partial}{\partial x_i} [n_i P \delta(f) \nabla f] + \frac{\partial}{\partial t} [\rho v_n \delta(f) \nabla f] \quad (5)$$

where p' is the sound pressure, n_i is the surface normal vector, v_n is the normal velocity, c is the sound velocity, and T_{ij} is the Lighthill stress tensor. As always, all of the variables are expressed in the appropriate units. The three terms on the right side of the equation represent quadrupole, dipole, and monopole generating waves, respectively. This equation allows the calculation of sound pressure in space.

2.3. Acoustic Post Processing

The obtained sound pressure of the monitoring point is a pressure fluctuation signal that changes with time. The time-domain sound pressure is converted into a frequency-domain sound pressure by Fast Fourier Transform (FFT):

$$P(f) = \int_{-\infty}^{+\infty} p(t) e^{-i2\pi f t} dt \quad (6)$$

Through the logarithmic operation to the sound pressure after the FFT operation, the sound pressure level result of the monitoring point can be obtained:

$$SPL(dB) = 10 \log_{10} \left[\frac{P(f)}{P_{ref}} \right]^2 \quad (7)$$

where P_{ref} is the reference sound pressure related to the minimum sound pressure amplitude that can be heard by a human, and the value is 2×10^{-5} Pa.

3. Simulation Model

3.1. Geometric Modeling

In this work, a heavy commercial vehicle was taken as the research object to study the sunroof buffeting noise. The size of the sunroof was 470 mm \times 670 mm. To better simulate the actual characteristics of the cab, a geometric model with a proportion of 1:1 to the actual vehicle was established, as shown in Figure 1. On the premise of not affecting the simulation accuracy, the door handles and the lamp of the commercial vehicle were simplified. Important interior decorating pieces such as berths, seats, and other relevant parts were retained.

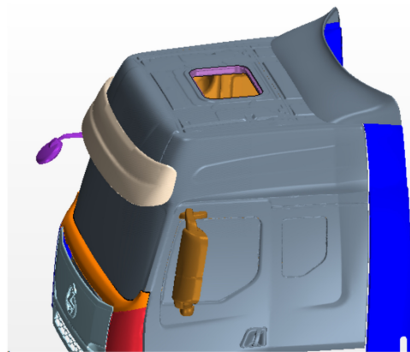


Figure 1. Geometric model of the commercial vehicle cab.

Assuming that the length, width, and height of the cab are L , W , and H , respectively, the virtual wind tunnel is a box that surrounds the cab model, and the size parameters were $20L$, $5W$, and $6H$, respectively. The distance from the inlet of the virtual wind tunnel to the front end of the cab, the side of the virtual wind tunnel to the side, and to the top of the cab, were $3L$, $2W$, and $4H$, respectively, as shown in Figure 2.

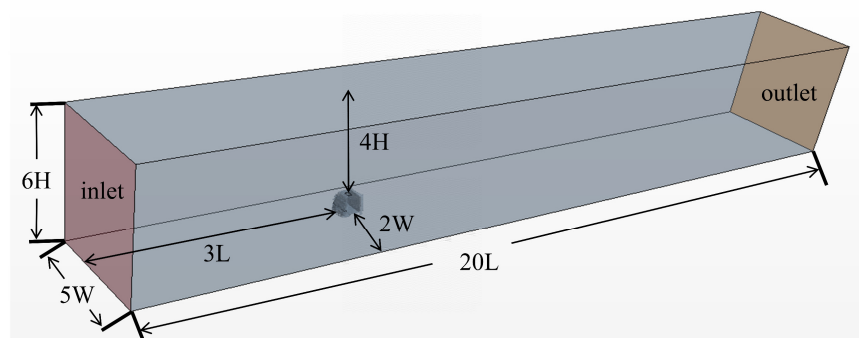


Figure 2. The wind tunnel calculation domain.

The pre-processing module of STAR-CCM+ software (Version 12.06, Siemens Digital Industries, Berlin, Germany) was used to mesh the cab and virtual wind tunnel. The cab

and the wall were divided into different size surface elements, which ranged from 10 to 250 mm. Solid elements were generated according to the surface elements. At the same time, six boundary layer elements were stretched on the surface of the cab to simulate the flow characteristics of the surface of the cab, and the size of the innermost elements was 0.25 mm. A monitoring point was set at the driver's right ear to record the pressure pulsation of the sunroof buffeting. Figure 3 is a partial mesh schematic diagram of the middle section of the cab and the virtual wind tunnel.

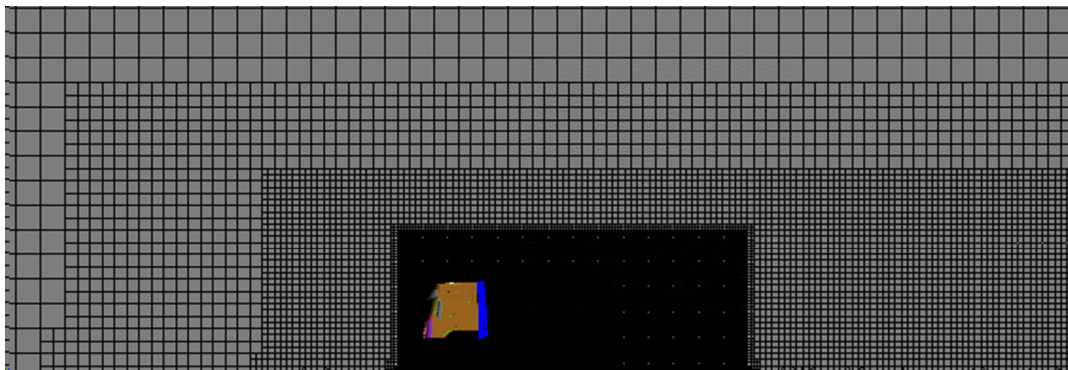


Figure 3. Partial mesh schematic diagram of the middle section.

3.2. Boundary Condition Setting

Due to the fact that the established wind tunnel model was a limited simulation area, it was necessary to set the model boundary conditions to make the simulation conform to the actual physical conditions. The model boundary conditions in this paper were set as follows.

- (1) The virtual wind tunnel inlet speed was set according to different working conditions.
- (2) The outlet pressure of the virtual wind tunnel was 0 Pa. At this time, the outlet pressure was equal to the atmospheric pressure.
- (3) The cab and computing domain ground was a non-slip wall.
- (4) The upper and the sidewall in the virtual wind tunnel were the free slip walls.

In the transient simulation process of the wind buffeting noise of skylights, the stationary solution of the finite element model was first calculated according to the turbulence model, and then the stationary solution was used as the initial value of the transient simulation. In this paper, the SST- $\kappa\omega$ turbulence model (a two-equation eddy-viscosity model) was used in the steady-state calculation process, the coupling numeration of velocity field and stress was based on the SIMPLE algorithm (a numerical procedure frequently used to solve the Navier–Stokes equations), and the discretization was second-order upwind. In the transient calculation, the numerical solution was based on the Detached-Eddy Simulation (DES). The simulation time was 1 second, and the step length was 0.0005 s. Each step was iterated five times before the next iteration calculation.

4. Simulation Results and Analysis of Sunroof Buffeting Noise

The commercial vehicle cab with the sunroof open can be regarded as a Helmholtz resonance cavity. The resonance frequency can be obtained according to the formula of the Helmholtz resonant cavity [19]:

$$f_v = \frac{c}{2\pi} \sqrt{\frac{A}{V \left(h + \frac{\pi}{2} \bullet \frac{D_h}{2} \right)}} \quad (8)$$

where c is the speed of sound, A is the area of the skylight, V is the cavity volume, h is the thickness of the skylight, and D_h is hydraulic diameter of the skylight, all of which are expressed in appropriate units. According to the geometry dimensions of the cab, it

was found that the resonance frequency of the cab cavity was 18.4 Hz. The actual driving feedback of the commercial vehicle showed that there was a strong sunroof buffeting noise at a speed of 70 km/h when the sunroof was opened. According to the established model, the sunroof buffeting noise of a commercial vehicle with a different inlet wind speed was analyzed, and the formation of the sunroof buffeting noise was studied to provide a guideline for the optimization of the sunroof buffeting noise of commercial vehicles.

4.1. Working Condition One

The buffeting noise of the sunroof with an inlet wind speed of 70 km/h was studied. Figure 4 shows the pressure pulsation results of the monitoring point. It can be seen that the amplitude of the pressure pulsation was increasing until 0.6 seconds. Although the sound pressure of the monitoring point was periodic, the flow field inside and outside the cab was not in a steady-state at this time. The pressure pulsation began to stabilize after 0.6 s. According to the pressure pulsation results in Figure 4, the lowest pressure value in the cab was around -240 Pa. Performing the FFT transformation on the pressure pulsation of the monitoring point makes it possible to obtain the spectrum as a result. Figure 5 shows the sound pressure level spectrum of the monitoring point after the FFT transformation. It can be seen that the maximum sound pressure level at the monitoring point was 111.5 dB and the corresponding frequency was 17.8 Hz while the sunroof was opened, and the inlet speed was 70 km/h. The simulation results are consistent with the buffeting noise characteristics including the low frequency and high sound pressure levels. The buffeting noise frequency was close to the resonance frequency, and it can be inferred that the cab had a resonance response at the inlet speed of 70 km/h.

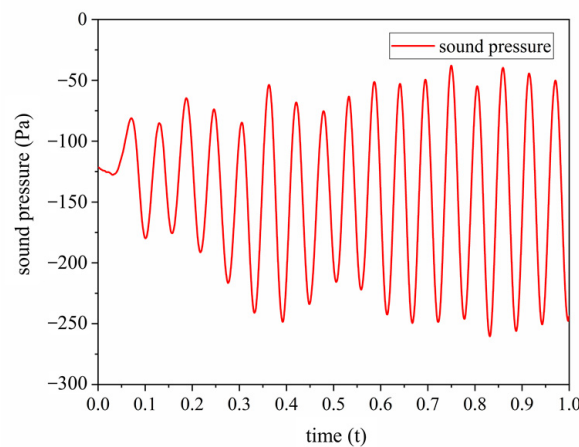


Figure 4. Pressure pulsation of the monitoring point while the inlet speed is 70 km/h.

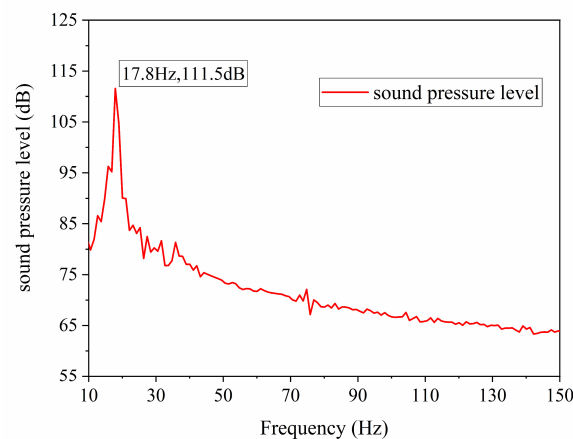


Figure 5. Sound pressure level spectrum.

The formation process of the buffeting noise of a sunroof with a speed of 70 km/h was studied. Figure 6 shows the color diagram of the transient pressure in the cab. In a commercial vehicle, the airflow separates on the forehead of the cab to produce turbulent vortices, which is different from that in the sedan. These vortices gradually become larger during the backward movement and fall off into the cab at the sunroof. The pressure wave generated by the turbulent vortex breaks causing the pressure in the cab to drop sharply.

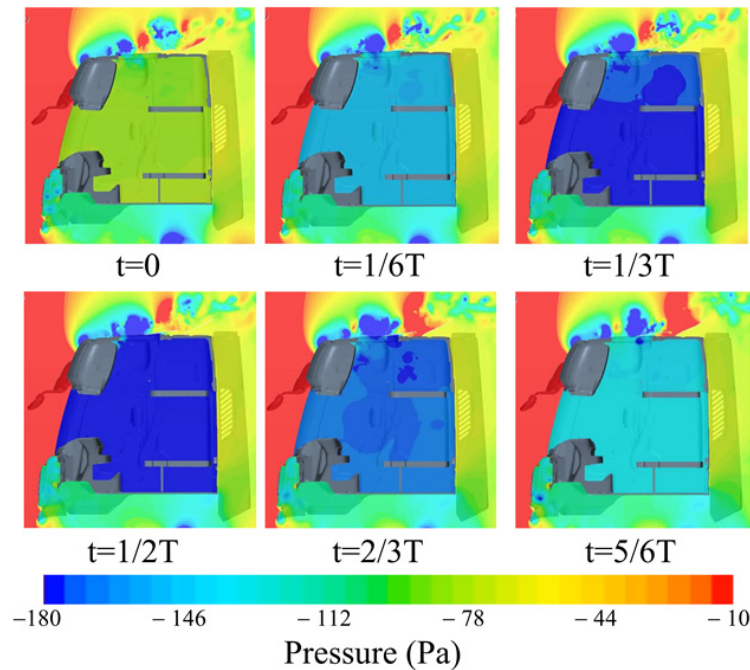


Figure 6. The transient pressure contour curve of the cab.

The process of the influence of the turbulent vortex on the sound pressure of the cab was analyzed in detail as follows. At $t = 0$, the low-pressure turbulence vortex was at the edge of the skylight and began to fall off into the cab. At this time, the pressure at the skylight area was lower than that in other areas. At $t = 1/6T$, the scale of the low-pressure turbulent vortex became larger. The turbulent vortex entered and broke in the cab, and the pressure wave generated by the breaking of the turbulent vortex in the cab made the pressure level in the cab drop significantly. The pressure wave spread through the entire cab, so the pressure gradient was very small. At $t = 1/3T$, the scale of the turbulent vortex continued to increase, and the turbulent vortex sustained shedding and breaking, reducing the pressure in the cab. At $t = 1/2T$, the impact of the shedding turbulent vortex on the indoor pressure reached the maximum, and the overall pressure level in the cab was less than -180 Pa. At $t = 2/3T$, it can be seen that the turbulent vortex moved to the rear edge of the skylight, the shedding effect of the turbulent vortex was weakened and the pressure in the cab rose. At the same time, a new small turbulent vortex was formed in front of the skylight. At $t = 5/6T$, the turbulent vortex moved away from the skylight with the airflow, and the pressure in the cab rose to a higher level. The scale of the new turbulent vortex expanded. Then the pressure state of the cab returned to the initial level, and at the same time the new turbulent vortex started a new process that affected the pressure in the cab.

4.2. Working Condition Two

To study the influence of different inlet wind speeds on the buffeting noise of the skylight, the inlet speed of the virtual wind tunnel was set to 60 km/h and the pressure fluctuation at the monitoring point was analyzed. Figure 7 shows the results of pressure pulsation at the monitoring point. It can be seen that, similar to the pressure pulsation at a speed of 70 km/h, the pressure pulsation was periodic. At the beginning of the simulation,

the amplitude of the pressure fluctuation of the monitoring point increased with time, and the pressure fluctuation tended to be stable after 0.75 s. The pressure pulsation of the monitoring point in condition two was transformed by FFT and compared with the frequency spectrum results of condition one. Figure 8 is the comparison result of the buffeting noise spectra. It can be seen that the maximum sound pressure level of condition two was 108.8 dB, which is lower than that of condition one by 2.7 dB. The corresponding frequency was 17.0 Hz, which is lower than that of condition one by 0.8 Hz. This means that reducing the inlet wind speed can improve the characteristics of the sunroof buffeting noise.

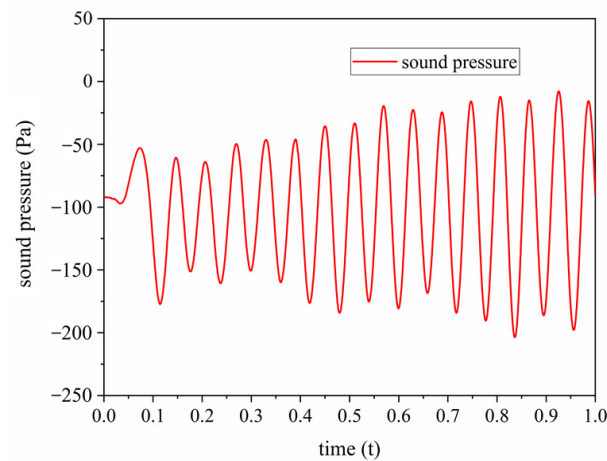


Figure 7. Pressure pulsation of the monitoring point while the inlet speed is 60 km/h.

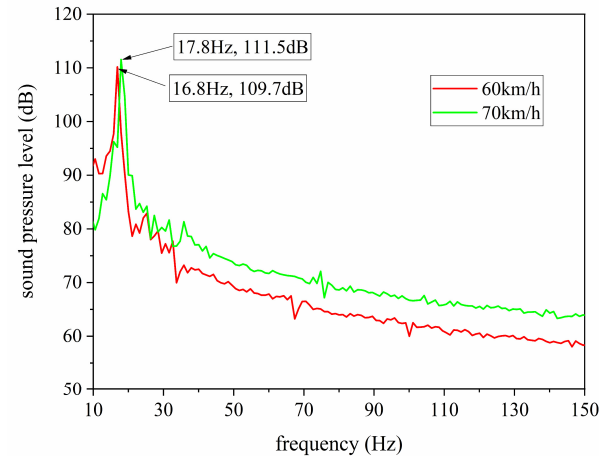


Figure 8. Comparison of spectra.

To study the impact of different inlet wind speeds on the sunroof buffeting noise in more detail, the cab forehead pressure contour curves of conditions one and two were analyzed. Figure 9 shows the comparison results of the forehead pressure contour curve when the inlet speeds were 70 km/h and 60 km/h, respectively. It can be seen that while the inlet wind speed was 70 km/h, the negative pressure area above the roof was larger than with a speed of 60 km/h. At the same time, reducing the inlet speed can help to reduce the low-pressure area at the forehead corner, which helps to weaken the turbulent vortex generated in the forehead. It can also be seen that while the inlet speed was 70 km/h, there were some small low-pressure turbulent vortices in the negative pressure area. These small low-pressure turbulent vortices can merge with the large turbulent vortex while moving with the airflow. The influence of the large turbulent vortex on the cab pressure will be enhanced.

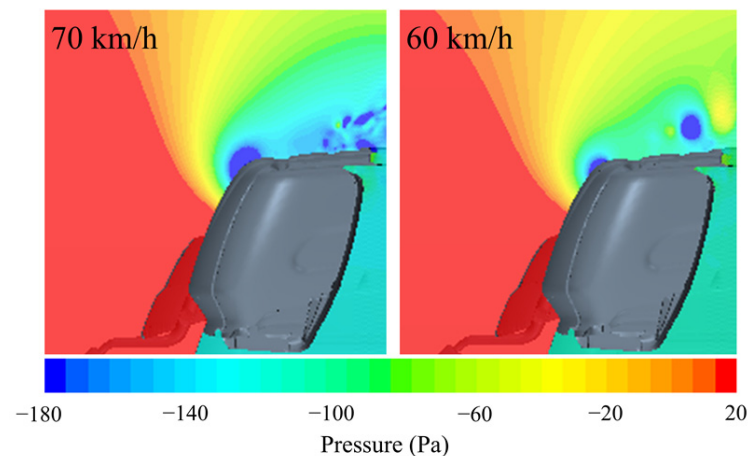


Figure 9. The pressure contour curve of the cab forehead with different speed.

Figure 10 is a contour curve of the cab pressure when the inlet speed was 60 km/h. It can be seen that the turbulent vortex did not fall into the cab while it moved through the sunroof but continued to move backward with the airflow, which is the reason why the pressure fluctuation decreased while the inlet speed was 60 km/h. The simulation results show that improving the flow field characteristics above the cab has a good effect on reducing the sunroof buffeting noise.

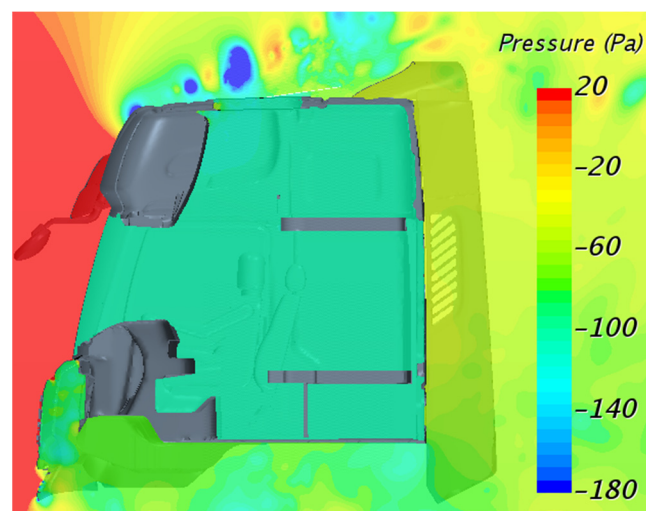


Figure 10. The pressure contour curve of the cab at 60 km/h.

5. Sunroof Buffeting Noise Control

There are two ways to reduce sunroof buffeting noise, including active control [20] and passive control [21]. The active control method requires the development of an active sound control device, which is more expensive to implement in practice. The passive control method is used to reduce the buffeting noise by designing the control structure. The passive control method is easy to implement and widely used in practice. After comprehensive consideration, the passive control alternatives were adopted in the current study to reduce the buffeting noise.

5.1. Optimization Scheme

From the comparative results of the sunroof buffeting noise with different inlet speeds, it can be seen that the flow field characteristics in the cab forehead area are complex at the inlet speed of 70 km/h, and there will be a smaller turbulent vortex. Since the commercial

vehicles studied are already mass-produced, optimizing the forehead of the cab will vastly increase the economic costs, particularly in relation to the installation of a small spoiler in front of the sunroof. The principle is to use the spoiler to change the flow field so as to prevent the turbulent vortex falling into the cab. However, installing a small spoiler increases parts and costs. It is proposed that the existing accessories including the sunshade and roof dome on the cab should be optimized to suppress the sunroof buffeting noise. The optimization content includes the installation angle of the sun visor and the shape of the roof dome. Adjusting the flow field at the forehead position by optimizing the sun visor reduces the turbulent vortex that is generated. By optimizing the roof dome, the lifting effect of the roof dome on the airflow is improved, so as to better guide the turbulent vortex away from the cab and to avoid the turbulent vortex falling off at the skylight. The specific design scheme is shown in Figure 11.

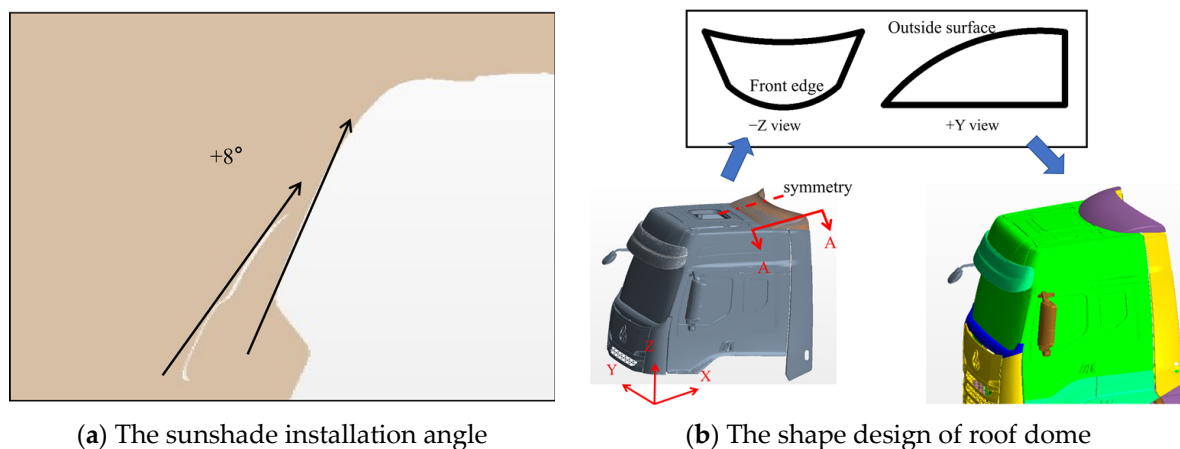


Figure 11. Optimal design of cab accessories.

Figure 11a is the schematic diagram of the installation angle of the sun visor. The installation angle is optimized based on the original sun visor, and the new installation angle is increased by 8. Figure 11b is the optimized schematic diagram of the roof dome. The roof dome is symmetrical about the center plane, and the shape optimization is explained with half of the roof dome. The optimization content includes the following steps: removing the upward edge of the original sun visor, adjusting the front end of the roof dome to a circular arc, and reducing the distance between the roof dome and the sunroof. The upper surface of the roof dome is changed to a convex arc surface. The height of the roof dome at the symmetrical plane is the same as that of the original roof dome. For this commercial vehicle, the corresponding height at the A-A section of the original car's roof dome is reduced by a 1/3, and the height after optimization is 110 mm. The roof dome between the symmetrical section and the A-A section is connected by a circular arc surface.

5.2. Buffeting Noise Simulation of the Optimized Scheme

The sunroof buffeting noise of the cab after the optimization of the sun visor and roof dome was analyzed. The inlet speed was 70 km/h. Figure 12 shows the pressure color map of the forehead before and after optimization. It can be seen that the scale of the negative pressure area above the roof and at the forehead corner decreased, which suppresses the phenomenon of the small vortex generated at the forehead. The position of the turbulent vortex above the roof is also improved. Figure 13 shows the sound pressure level spectra of the monitoring point before and after optimization. It can be seen that the optimization scheme can effectively improve the flow field characteristics above the roof. The sound pressure level at the monitoring point decreased by 6%, from 111.5 dB to 104.8 dB, meaning that the sunroof buffeting noise has been reduced.

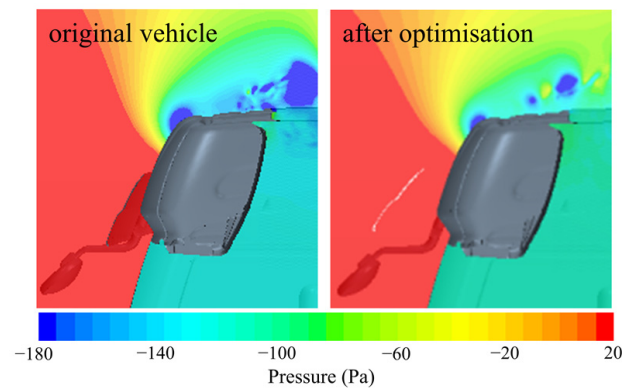


Figure 12. The pressure contour curve of the cab forehead before and after optimization.

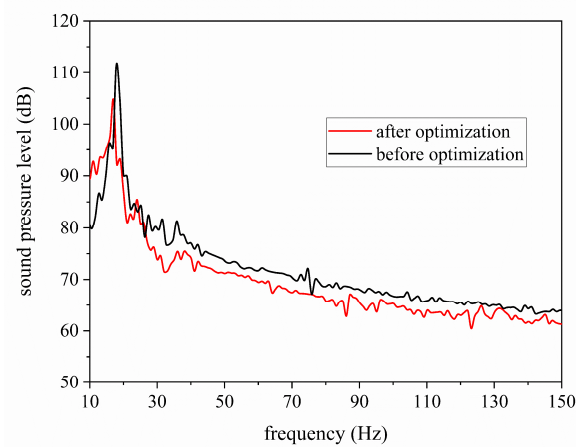


Figure 13. The sound pressure level spectra before and after optimization.

5.3. Wind Resistance Analysis

The wind resistance of the commercial vehicle after the optimization of the sun visor and roof dome accessories was analyzed. The analysis model added the main structural components of commercial vehicles including a trailer, wheels, and other parts. Table 1 shows the wind resistance coefficients of the commercial vehicle. Figure 14 is the color diagram of the surface pressure of the commercial vehicle before and after optimization when the inlet wind speed was 70 km/h.

Table 1. Wind resistance coefficients of the commercial vehicles.

	Wind Resistance Coefficient (C_d)	Change Rate
Original car	0.581	-
After optimization	0.572	-1.55%

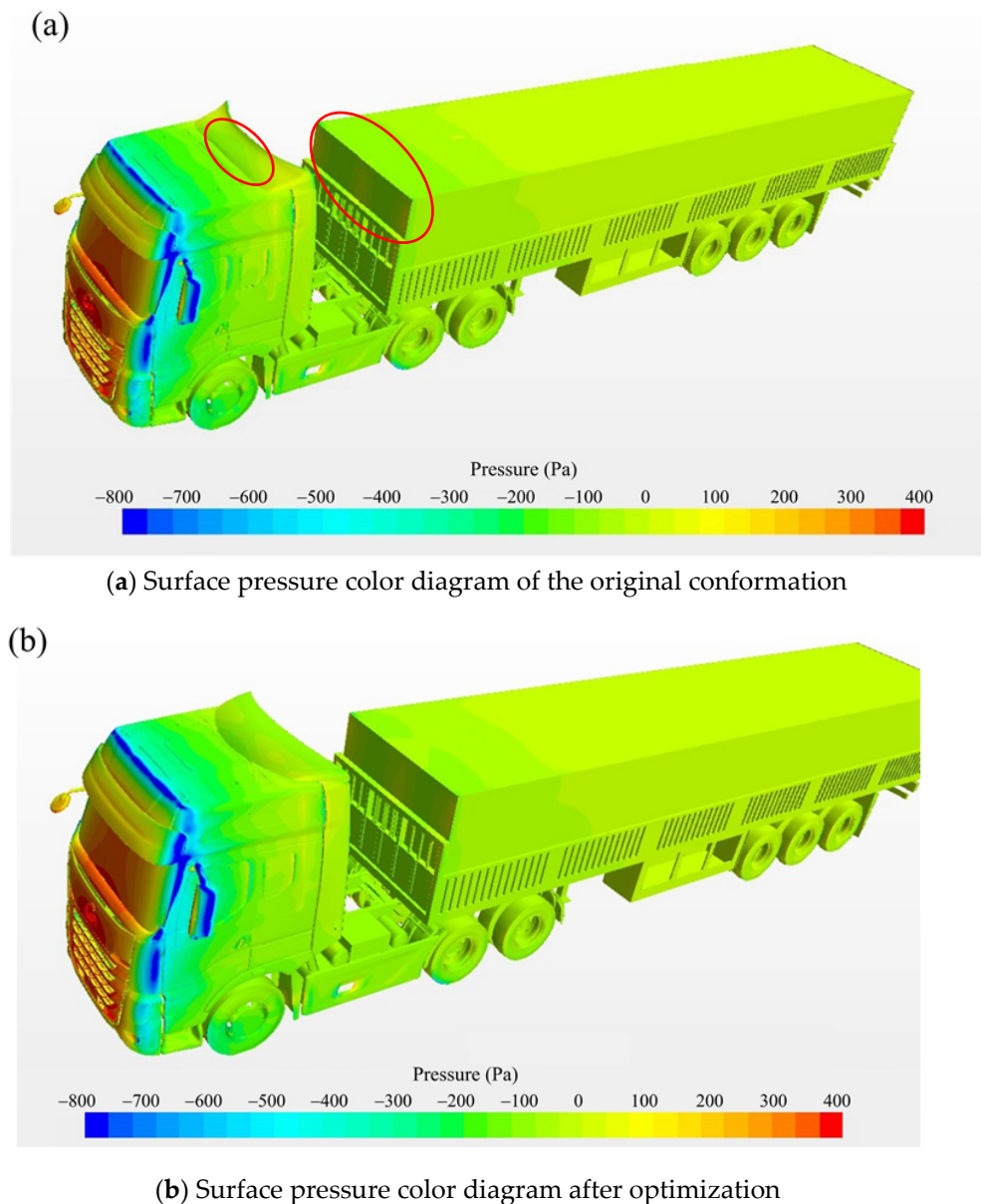


Figure 14. Surface pressure of commercial vehicles before and after optimization.

It can be seen from Table 1 that after the optimization of the installation angle of the sun visor and the shape of the roof dome, the wind resistance coefficient of the commercial vehicle was reduced by 1.55% compared with the original vehicle. In the original car, there was a negative pressure area in the middle of the roof dome, which was caused by the airflow above the roof. Affected by the tail vortex behind the cab, there was also a large negative pressure area at the front end of the trailer. After the optimization of the sun visor and roof dome, the surface pressure of the roof dome and the trailer increased due to the improvement of the airflow characteristics above the roof and the trailing vortex behind the cab, which achieves the target of reducing the pressure resistance of the commercial vehicle.

5.4. Sunroof Buffeting Noise Test

A road test was carried out on the sunroof buffeting noise of a commercial vehicle with the sunroof fully opened. The test was carried out on a highway with asphalt pavement, using the Test.Lab noise test equipment, and the vehicle speed was 70 km/h. The weather was fine, the wind speed was less than 3 m/s, and the environmental noise was less than 40 dB. Figure 15 shows the test equipment and the opening skylight. The sound pressure

level near the driver's right ear was measured, and the results are shown in Table 2. It can be seen that after the optimization of the sun visor and roof dome accessories, the sunroof buffeting noise of the commercial vehicle was reduced from 116.3 dB to 109.2 dB, a decrease of 7.1 dB. The results of the simulation and the experiment are relatively close, indicating the effectiveness of the optimization scheme.

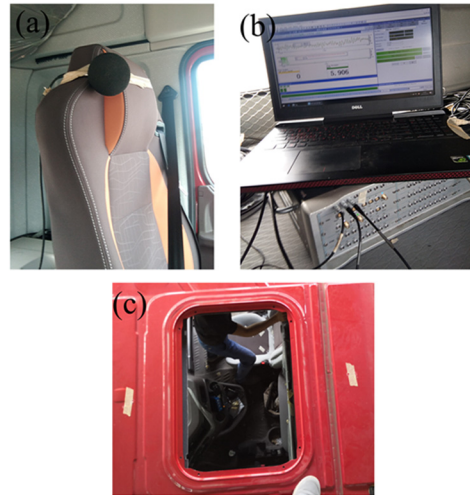


Figure 15. Sunroof buffeting noise test. (a) microphone. (b) test.lab noise test system. (c) the full opening skylight.

Table 2. Comparison of sunroof buffeting noise results.

	Before Optimization		Optimized	
	Frequency (Hz)	Sound Pressure Level (dB)	Frequency (Hz)	Sound Pressure Level (dB)
Simulation	17.8	111.5	17.0	104.8
Test	16.5	116.3	16.1	109.2

6. Conclusions

This work focused on heavy commercial vehicles to study the sunroof buffeting noise. The existing accessories including the sun visor and the roof dome were optimized to improve the flow field characteristics of commercial vehicles to reduce the sunroof buffeting noise and wind resistance coefficient. The main conclusions were:

- (1) Based on numerical simulations, the airflow separates on the forehead of the cab to produce turbulent vortices. These vortices gradually become larger during the backward movement and fall off into the cab at the sunroof. The pressure wave generated by the turbulent vortex breaks causing the pressure in the cab to drop sharply. Turbulent vortices have periodic characteristics.
- (2) After analyzing the sunroof buffeting noise for two-speed conditions, it was evidenced that reducing the speed can improve the flow field characteristics above the roof and reduce the number of the small turbulent vortices.
- (3) Optimizing the sun visor and roof dome accessories of the cab can reduce the sunroof buffeting noise. The validity of the simulation results was verified through experiments.
- (4) The optimization scheme of the sun visor and roof dome improves the flow field characteristics of the commercial vehicles. This scheme reduces the impact of airflow on the roof dome and the local pressure drag and reduces the aerodynamic drag coefficient of the commercial vehicle, improving fuel economy, and the design cost is also reduced.

All of the above can be considered of relevance in this field of research and should be further explored.

Author Contributions: Conceptualization and funding acquisition, R.T.; methodology, H.H.; software, Z.L.; writing—original draft preparation, S.L.; validation, E.X.; formal analysis, F.X.; writing—review and editing, A.N.-D. All authors have read and agreed to the published version of the manuscript.

Funding: This work was supported by the National Natural Science Foundation of China (No. 52065013), the Guangxi Youth Science Fund Project (2018GXNSFBA281012), the Innovation-Driven Development Special Fund Project of Guangxi (Guike AA19182004), and the Liuzhou Scientific Research and Planning Development Project (2018AA20301).

Institutional Review Board Statement: Not applicable.

Informed Consent Statement: Not applicable.

Data Availability Statement: Not applicable.

Conflicts of Interest: The authors declare no conflict of interest.

References

- Zhang, Q.; He, Y.; Wang, Y.; Xu, Z.; Zhang, Z. Computational study on the passive control of sunroof buffeting using a sub-cavity. *Appl. Acoust.* **2020**, *159*, 1–9. [\[CrossRef\]](#)
- Chen, S.; Wang, D.; Liang, J. Sound quality analysis and prediction of vehicle interior noise based on grey system theory. *Fluct. Noise Lett.* **2012**, *11*, 1–22. [\[CrossRef\]](#)
- Lemaitre, G.; Vartanian, C.; Lambourg, C.; Boussard, P. A psychoacoustical study of wind buffeting noise. *Appl. Acoust.* **2015**, *95*, 1–12. [\[CrossRef\]](#)
- He, Y.; Long, L.; Yang, Z. A study on wind tunnel test on side window buffeting characteristics of a sedan. *Automot. Eng.* **2017**, *39*, 1011–1017.
- Yang, Z.; Gu, Z.; Tu, J.; Dong, G.; Wang, Y. Numerical analysis and passive control of a car side window buffeting noise based on scale-adaptive simulation. *Appl. Acoust.* **2014**, *79*, 23–34. [\[CrossRef\]](#)
- Oettle, N.; Meskine, M.; Senthoooran, S.; Bissell, A.; Balasubramanian, G.; Powell, R. A computational approach to assess buffeting and broadband noise generated by a vehicle sunroof. *SAE Int. J. Passeng. Cars Mech. Syst.* **2015**, *8*, 196–204. [\[CrossRef\]](#)
- Wang, Y.; Deng, Y.; Yang, Z.; Jiang, T.; Su, C.; Yang, X. Numerical study of the flow-induced sunroof buffeting noise of a simplified cavity model based on the slightly compressible model. *Proc. Inst. Mech. Eng. Part D* **2013**, *227*, 1187–1199. [\[CrossRef\]](#)
- Wang, Z.; Zhuang, M. A numerical study of trailing edge serrations on sunroof buffeting noise reduction. *SAE Int. J. Veh. Dyn. Stab. NVH* **2017**, *1*, 112–118. [\[CrossRef\]](#)
- Gu, Z.; Zong, Y.; Luo, Z.; Yang, Z.; Jiang, C.; Chen, Z. Numerical simulation of automobile side-window buffeting noise based on fluid–structure interaction. *Appl. Acoust.* **2015**, *90*, 126–137. [\[CrossRef\]](#)
- Gong, X.; Wang, J.; Deng, C.; Wei, P.; Liu, B.; Li, L. Optimization and simulation of SUV sunroof buffeting noise. In Proceedings of the Society of Automotive Engineers (SAE)—China Congress, Shanghai, China, 26–28 October 2016; Springer: Singapore, 2016; pp. 365–373.
- He, Y.; Zhang, Q.; An, C.; Wang, Y.; Xu, Z.; Zhang, Z. Computational investigation and passive control of vehicle sunroof buffeting. *J. Vib. Control* **2020**, *26*, 747–756. [\[CrossRef\]](#)
- He, Y.; Zhang, Q.; Xu, Z.; Zhang, Z. Study on the sunroof buffeting suppression with a notched flat deflector. In Proceedings of the INTER-NOISE and NOISE-CON Congress and Conference Proceedings, Madrid, Spain, 16–19 June 2019; Institute of Noise Control Engineering: Reston, VA, USA, 2019; Volume 259, pp. 1677–1683.
- He, Y.Z.; Long, L.H.; Yang, Z.G. Reduction and optimization of a vehicle’s rear side window buffeting. *Noise Control Eng. J.* **2018**, *66*, 298–307. [\[CrossRef\]](#)
- Hu, X.J.; Peng, G.; Zhang, Y.H.; Mao, J.M.; Sun, X.Z.; Sang, T.; Lan, W.; Wang, J.Y. Buffeting noise characteristics and control of automobile side window. *SAE Int. J. Veh. Dyn. Stab. NVH* **2021**, *5*, 65–79. [\[CrossRef\]](#)
- Gu, Z.Q.; Liu, Z.Z.; Yang, Z.D.; Zheng, L.D.; Yin, S.B. Optimization of air-jet structure for automobile wind buffeting noises. *China Mech. Eng.* **2021**, *32*, 681–733.
- Chen, Z.; Wen, G.; Li, W. Influence of stream velocity on the buffeting characteristic of vehicle sunroof. *Automot. Eng.* **2013**, *35*, 654–659.
- Zhang, Y.; Zhang, J.; Li, T.; Zhang, L. Investigation of the aeroacoustic behavior and aerodynamic noise of a high-speed train pantograph. *Sci. China Technol. Sci.* **2017**, *60*, 561–575. [\[CrossRef\]](#)
- Slaboch, P.; Ma, R.; Shannon, D.; Gleason, M.; Puskarz, M. Window buffeting measurements of a full scale vehicle and simplified small scale models. *SAE Int. J. Passeng. Cars* **2009**, *2*, 410–418. [\[CrossRef\]](#)
- Wu, H.; Zhou, J.; Chen, Q.; Liu, G.; Qian, C. A study on rear window wind vibration of a sedan. *Automob. Technol.* **2016**, *9*–25.

-
20. Kook, H.-S.; Shin, S.-R.; Cho, J.; Ih, K.-D. Development of an active deflector system for sunroof buffeting noise control. *J. Vib. Control*. **2014**, *20*, 2521–2529. [[CrossRef](#)]
 21. Wang, Y.; Lee, H.C.; Li, K.M.; Gu, Z.; Chen, J. Experimental and numerical study of flow over a cavity for reduction of buffeting noise. *Acta Acust. United Acust.* **2012**, *98*, 600–610. [[CrossRef](#)]